PCP
PLANT & CELL PHYSIOLOGY

Different Types Domains are Present in Complex I from Immature Seeds and of CA Adult Plants in *Arabidopsis thaliana*

Juan Pablo Córdoba[1,2], Marisol Fassolari[1,2], Fernanda Marchetti[1], Débora Soto[1], Gabriela C. Pagnussat[1] and Eduardo Zabaleta[1,*]

[1]Instituto de Investigaciones Biológicas (IIB)-Universidad Nacional de Mar del Plata (UNMdP)-CONICET, Funes 3250 3er nivel, 7600 Mar del Plata, Argentina
[2]These authors contributed equally to this work

*Corresponding author: E-mail, ezabalet@mdp.edu.ar; Fax, +54 223 475 30 30.
(Received October 4, 2018; Accepted January 10, 2019)

Regular Paper

Mitochondrial Nicotinamide adenine dinucleotide (NADH) dehydrogenase complex is the first complex of the mitochondrial electron transfer chain. In plants and in a variety of eukaryotes except Opisthokonta, complex I (CI) contains an extra spherical domain called carbonic anhydrase (CA) domain. This domain is thought to be composed of trimers of gamma type CA and CA-like subunits. In Arabidopsis, the CA gene family contains five members (CA1, CA2, CA3, CAL1 and CAL2). The CA domain appears to be crucial for CI assembly and is essential for normal embryogenesis. As CA and CA-like proteins are arranged in trimers to form the CA domain, it is possible for the complex to adopt different arrangements that might be tissue-specific or have specialized functions. In this work, we show that the proportion of specific CI changes in a tissue-specific manner. In immature seeds, CI assembly may be indistinctly dependent on CA1, CA2 or CA3. However, in adult plant tissues (or tissues derived from stem cells, as cell cultures), CA2-dependent CI is clearly the most abundant. This difference might account for specific physiological functions. We present evidence suggesting that CA3 does not interact with any other CA family member. As CA3 was found to interact with CI FRO1 (NDUFS4) subunit, which is located in the matrix arm, this suggests a role for CA3 in assembly and stability of CI.

Keywords: CA domain • Complex I • Embryogenesis • Gamma carbonic anhydrase • Plant mitochondria • Respiration.

Accession numbers: Sequence data from this article can be found in the Arabidopsis Genome Initiative or GenBank/EMBL databases under the following accession numbers: Arabidopsis CA1 (At1g19580), Arabidopsis CA2 (At1g47260), Arabidopsis CA3 (At5g66510), Arabidopsis FRO1 (At5g67590) and mitochondrial Arabidopsis ND6 (AtMg00270) and ND9 (AtMg00070).

Introduction

Mitochondrial complex I (CI also referred as Nicotinamide adenine dinucleotide (NADH) dehydrogenase or NADH: UbiquinoneOxidoreductase, EC 1.6.5.3) is the main entrance of electrons from metabolism to the mitochondrial electron transfer chain in the oxidative phosphorylation (OXPHOS) system. In all organisms, CI conforms an L-shaped structure with a peripheral arm towards the mitochondrial matrix and a membrane arm. In bacteria, the CI contains 14 subunits, called the core, which is conserved in all other organisms (Cardol 2011, Baradaran et al. 2013, Berrisford et al. 2016, Subrahmanian et al. 2016). However, other eukaryotic organisms contain a variable number of accessory subunits (ranging from 30 to 36), some of them involved in the assembly process of the complex (Stroud et al. 2016).

In plants and in a variety of eukaryotes except for Opisthokonta, CI contains an extra spherical domain named carbonic anhydrase (CA) domain, composed of putative gamma type CA subunits that are thought to be arranged in trimers (Dudkina et al. 2005). In Arabidopsis, these subunits are CA1, CA2 and CA3, which contain almost all the aminoacids of the active site conserved respect to the active gamma type CA from *Methanosarcina thermophila* (Parisi et al. 2004). In addition, other two subunits, CAL1 and CAL2 (for CA like) show less conservation (Perales et al. 2004). In all plants analyzed so far both CAs and CALs are present in their genomes (Perales et al. 2004, Peters et al. 2008, Klodmann et al. 2010).

The CA domain has been implicated in the assembly of CI (Perales et al. 2005) which was experimentally demonstrated by biochemical decortications of the complex (Klodmann et al. 2010) or by subcomplexes accumulation in CI mutants (Meyer et al. 2011). Recently, it was shown that the CA domain represents the initial step of CI assembly (Ligas et al. 2018). Overexpression of CA2 results in anther indehiscence,

Plant Cell Physiol. 60(5): 986–998 (2019) doi:10.1093/pcp/pcz011, Advance Access publication on 22 January 2019, available online at https://academic.oup.com/pcp

which has been related to low accumulation of reactive oxygen species (ROS) (Villarreal et al. 2009). Even when the CA activity could not be demonstrated so far, bicarbonate/CO_2 binding was experimentally shown for recombinant CA2 (Martin et al. 2009). Also, the CA domain has been associated with carbon recycling in the context of photorespiration. Mutants lacking CA2 and one of the CAL proteins show a photorespiratory phenotype (Soto et al. 2015). Recently, the CA domain has been also linked to plant embryogenesis (Córdoba et al. 2016, Fromm et al. 2016a, Fromm et al. 2016b, Fromm et al. 2016c, Ostersetzer-Biran 2016). Plants lacking two CA subunits (CA1 and CA2) exhibit embryo developmental defects although shrunken seeds are rescued in sucrose supplemented media. Unexpectedly, the fifth protein, CA3, had not been found in the 85 kDa CA domain (Klodmann et al. 2010), although a recent work reported the presence of this subunit within the assembly intermediate of 85 kDa through new complexome profiling techniques (Ligas et al. 2018).

In this work, we show that *ca1ca3* double mutants are embryo or seedling lethal as the *ca1ca2* knockout lines because CI is not assembled. Plants can be rescued using sucrose supplemented media, but they are severely affected. On the other hand, *ca2ca3* double knockout mutants are able to complete embryogenesis and germinate normally, although growth of these mutant plants is strongly compromised. They show a severe dwarf phenotype that cannot be completely rescued by high CO_2 concentration or sucrose supplementation, suggesting problems in respiration. Indeed, CI activity is very low. Since CA1 and CA2 do not interact, a model involving a CA1 dependent CI and a CA2 dependent CI was suggested where CA1-CA1-CAL trimers or CA2-CA2-CAL trimers allow the assembly of the entire complex (Córdoba et al. 2016). In this work, we show evidence that each type of CI is differently present depending on the plant life cycle stage/tissue. Thus, we propose that CA1 and CA2 dependent complexes I are indistinctly assembled in immature embryos, while CA2-dependent CI is clearly the most abundant in leaves. CA3 seems to be a constitutively component, since *ca3* mutant plants have lower NADH dehydrogenase (DH) activity than Col-0 in all stages analyzed. However, CA3 does not interact with any of the other four members of the family. In light of a recent publication where CA3 was found as a component of the 85 kDa intermediate (Ligas et al. 2018), we propose that this subunit is possibly forming homotrimers and also contribute to the assembly of the complex, particularly in early embryos where the expression of the *CA3* gene is increased. In addition, CA3 may interact with FRO1 (NDUFS4), a subunit present in the interface of the membrane and matrix arms. The *fro1* mutant lines show a dwarf phenotype and are able to assemble only the membrane arm of CI with no NADH DH activity (Kühn et al. 2015). Double mutant *ca3fro1* shows a significant increase in the number of unviable seeds from 5% in the single mutant to 20% in the double mutant. Altogether, our results suggest that CA3 might contribute to the assembly and stability of CI.

Results

Double *ca2ca3* mutants show low growth rate while double *ca1ca3* mutants are embryo/seedling lethal

The first described CA mutant with biochemical alterations was a T-DNA insertional mutant in the *CA2* gene of *Arabidopsis thaliana* showing a strong reduction of CI (Perales et al. 2005). However, any other single mutant affecting each one of the rest of the CA/CAL proteins do not show any altered phenotype in comparison to Col-0 plants, suggesting at least partial functional redundancy. Thus, with the aim to elucidate the physiological role of the CA domain, we thus performed crosses involving *ca3* mutants and other *ca* mutants in order to study its physiological role.

Double homozygous *ca2ca3* mutants show normal embryo development and germinate within a normal time frame. Nevertheless, plants are significantly smaller than Col-0 (**Fig. 1A**). Under a 12/12 L/D photoperiod, *ca2ca3* mutant plants flowered in average 9 d later than Col-0 (**Fig. 1B**), but showing the same number of rosette leaves at bolting. This phenotype could not be completely rescued by cultivation of plants under 2000 ppm CO_2 atmosphere or in MS medium supplemented with 3% w/v sucrose (Supplementary Fig. S2).

On the other hand, using the alleles described in M & M, double homozygous *ca1ca3* mutants could not be found in the progeny of selfed heterozygous *CA1ca1ca3ca3* plants. As this suggests a lethal combination, a silique analysis was performed. Indeed, siliques from *CA1ca1ca3ca3* plants contain a high proportion of small, white, immature seeds that shrunk as the siliques matured (**Fig. 2A**). The proportion detected was 24.95% in still green siliques and 19.74% in matured, dry siliques (Supplementary Fig. S3), which suggests embryo lethality. Indeed, white (delayed) and green embryos collected from *CA1ca1ca3ca3* siliques were genotyped, confirming double mutation in homozygosis (Supplementary Fig. S4). As occurred in *ca1ca2*, *ca1ca3* double mutant embryos show delayed embryogenesis, which is detectable 60 hours after pollination (HAP) (**Fig. 2B-VII**) (Córdoba et al. 2016). At about 240 HAP, while Col-0 embryos are completely developed (**Fig. 2B-V**), *ca1ca3* embryos are found at late torpedo/curled cotyledon stage without greening (**Fig. 2B-X**).

Double mutant *ca1ca3* embryos show low mitochondrial membrane potential

As a low amount of CI negatively affects mitochondrial membrane potential (MMP) (Córdoba et al. 2016), MMP was measured using TetraMethylRodhaMine probe (TMRM) on developing mutant and Col-0 embryos. After controlled manual pollination, embryos were extracted at different developmental stages from Col-0 and *CA1ca1ca3ca3* siliques and stained with TMRM. In normal active mitochondria, TMRM staining results in intense red fluorescence (**Fig. 3A–D**). When embryos from *CA1ca1ca3ca3* siliques were analyzed around 60 HAP (**Fig. 3F**), 23.2% ($N = 65$) of embryos show

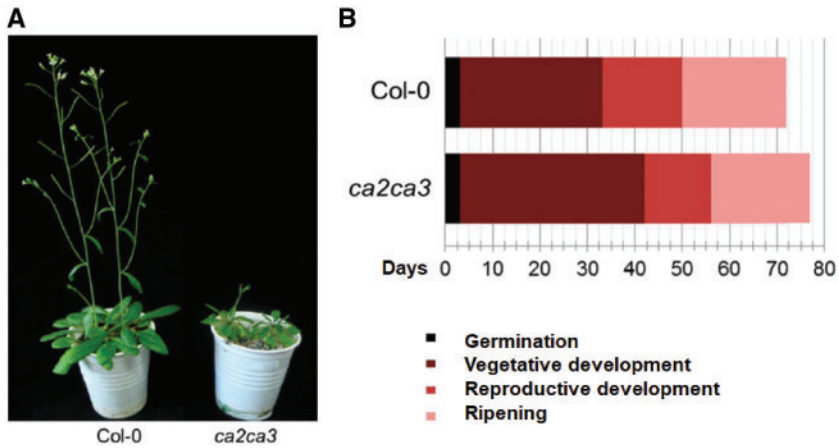

Fig. 1 *ca2ca3* double null mutant shows lower growth rate than Col-0 plants. Col-0 and *ca2ca3* double mutant plants were cultivated under 12/12 h L/D light conditions. (A) Double mutant plants are, in average, smaller than Col-0 43 d after germination. (B) *ca2ca3* shows lower growth rate and extended life cycle. Flowering takes 9 d more than in Col-0, but with the same number of leaves.

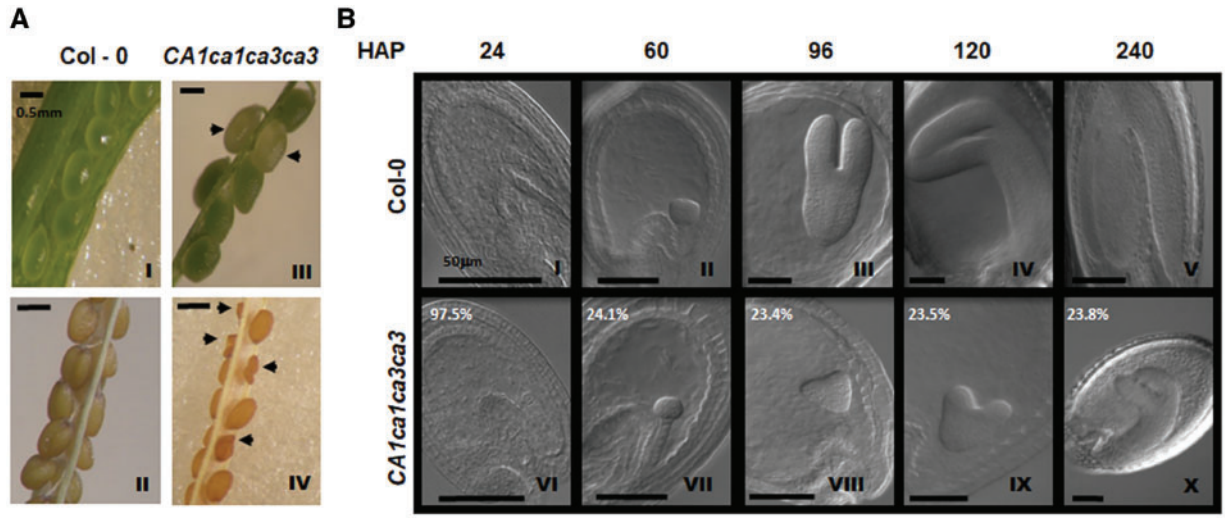

Fig. 2 *ca1ca3* double null mutation is embryo lethal. (A) *ca1ca3* siliques show abnormal seeds. In immature siliques (I and III), double homozygous embryos are still pale (arrowheads). In mature siliques (II and IV), the mutant ones are shrunken (arrowheads). Bars: 0.5 mm. (B) Embryos within pale seeds are delayed in their development. Percentages indicate the proportion of observed embryos in that stage. Bars: 50 mm.

evident low MMP levels (about 70% lower than Col-0). At later stages (around 90 HAP), embryos displaying low fluorescence show developmental delay (24.4% from total embryos in the siliques; $N = 53$ embryos; **Fig. 3G**). Notably, around 120 HAP, *ca1ca3* embryos (which are still delayed) recover their MMP at levels comparable to the ones observed in Col-0 embryos (25.7%, $N = 58$; **Fig. 3H**). Normal MMP levels are maintained until the end of embryogenesis (240 HAP).

CA1 and *CA3* promoters are active during embryo development

Putative promoter regions of the genes of interest were cloned upstream the *uidA* (b-glucuronidase GUS) reporter gene to determine their transcriptional activity. A region covering 2,000 base pair (BP) upstream of the first translational ATG codon of *CA1* was used. High promoter activities were found during pollen development while no activity was observed in embryo sac (**Fig. 4A, B**). Gus staining was evident in the developing embryo, from globular to heart stages (**Fig. 4C–F**). GUS activity was not detected in mature green (final stage) embryos although peripheral endosperm seems to have some *CA1* promoter activity (**Fig. 4H**).

To assay *CA3* promoter activity, 1,470 base pairs upstream of the first translational ATG of *CA3* were also fused to the *uidA* (GUS) reporter gene. Although there is no detectable activity at very early stages of embryo development (zygote to preglobular stages **Fig. 4J**), strong GUS activity was detected at late globular to heart stages (pale embryos, **Fig. 4K, L**).

Since the *CA2* gene is highly expressed at the end of embryogenesis (green embryos, Córdoba et al. 2016), all three CA genes seem to have a complementary expression pattern during embryogenesis.

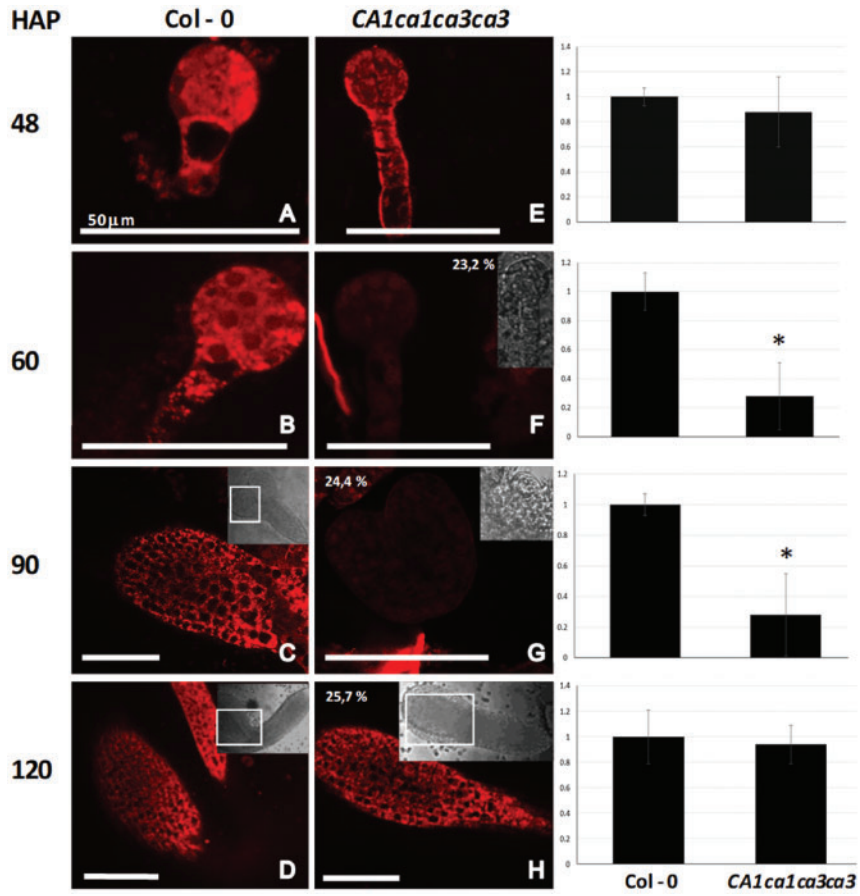

Fig. 3 Delayed *ca1ca3* embryos have low MMP. Col-0 and *ca1ca3* embryos were incubated with tetra-methyl-rhodamine after different HAP as indicated. Embryos were then analyzed using confocal microscopy. Within mutant *CA1ca1ca3ca3* siliques, there are around 25% of delayed embryos, which show low MMP. Membrane potential drops around 60 HAP in delayed embryos (F), but there are not differences with Col-0 at 120 HAP (H). Right column plots show red fluorescence relative to Col-0. Asterisks mean statistically significant difference analyzed by T-test ($P < 0.05$). Percentages indicate the proportion of embryos observed at each stage. Upper right pictures in C, D, F, G and H indicate bright field images and the region shown using confocal microscopy. Bars: 50 µm.

ca1ca3 seedlings do not survive under normal growth conditions

Shrunken seeds obtained from *CA1ca1ca3ca3* self-pollinated plants germinate about 9 d after sowing in MS medium or soil, although seedlings die 2 d later. However, if these double mutant seeds are sown in MS medium supplemented with 1% w/v sucrose, double mutant *ca1ca3* seedlings are able to survive. The same result was observed when seedlings were growing under long- or short-day conditions. However, 2 weeks after sowing (11 d if growing under long-day conditions) is necessary to transfer the plants to a medium containing 3% w/v sucrose for the plants to survive. Even when *ca1ca3* double homozygous plants are able to grow on plates supplemented with sucrose, they are severely affected, looking smaller and showing bleached leaves (**Fig. 5A**). Fifteen days after growing in these conditions, plants were transferred to soil. After 21 d, *ca1ca3* plants look healthier (**Fig. 5B**), although they show a notable developmental delay taking into account that Col-0 plants grown during the same period of time (47 d) under the same conditions are at ripening stage (**Fig. 5B**). Rescued plants were confirmed to be double homozygous for the mutated alleles by genotyping (Supplementary Fig. S5A). Further quantitative Reverse Transcriptase-Polymerase Chain Reaction (qRT-PCR) analyses show extremely low transcript levels of *CA1* and *CA3* genes in those plants (Supplementary Fig. S5B). Rescued plants are able to produce few seeds (5–10 seeds per silique); however, they are all shrunken and do not germinate, even in sucrose-supplemented media (Supplementary Fig. S5C). Moreover, alternative oxidases are induced in *ca1ca3* rescued plants (Supplementary Fig. S6), and they also accumulate ROS as hydrogen peroxide and superoxide anion (**Fig. 5C**).

CI is not detected by Coomasie blue staining in the *ca1ca3* mutants

Cell suspension cultures derived from *ca1ca3* rescued plants were established. In order to study the OXPHOS composition of this mutant, mitochondria were isolated, and their membrane proteins were solubilized. Proteins were then separated in 2D Blue Native/sodium dodecyl maltoside-Polyacrylamide Gel Electrophoresis (BN/SDS-PAGE) gels. The comparison between Col-0 (**Fig. 6A**) and *ca1ca3* (**Fig. 6B**) proteomes reveals that CI and $I+III_2$ supercomplex could not be detected in

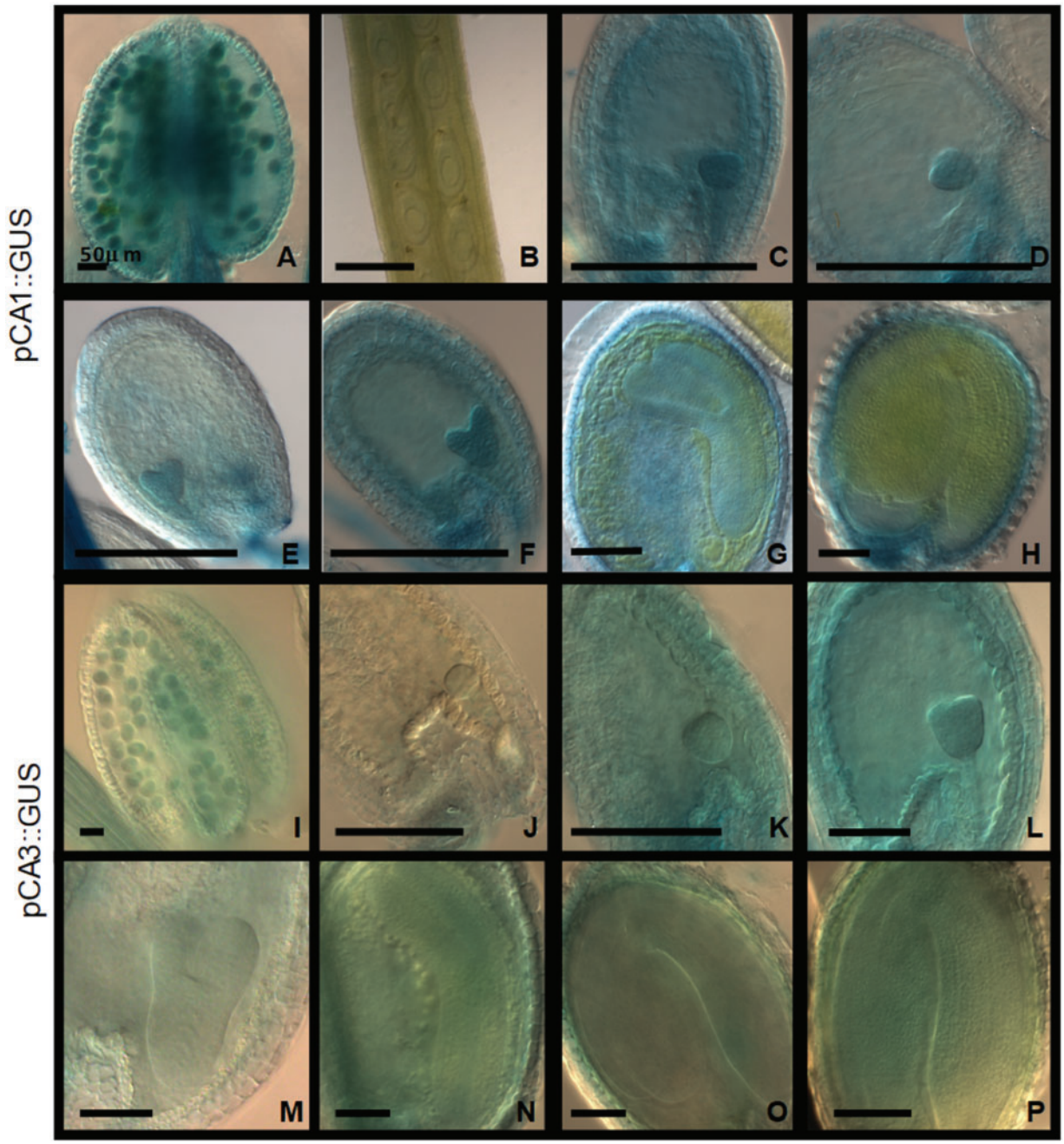

Fig. 4 *CA1* and *CA3* promoter regions are mainly active during early stages of embryogenesis. Two thousand and 1047 base pairs upstream the first translational ATG codon from *CA1* and *CA3* genes (respectively) were transcriptionally fused to the GUS reporter gene and introduced into Col-0 plants by floral dip. Siliques at different stages were manually opened and incubated with X-gluc in an appropriate buffer overnight. After incubation, samples were mounted on slides and cleared with Hoyer's solution. Stages: (A, I) anther showing stained microgametophytes; (B) ovules; (C, K) globular; (D) early heart; (E, L) heart; (F) late heart; (G, N) late torpedo (curled cotyledon); (H, O and P) mature green; (J) early globular; (M) torpedo. Bars: 50 µm.

ca1ca3 mitochondria. None of the normal CI subunits were observed in the second dimension and NADH DH activity could not be detected in *ca1ca3* mitochondrial protein complexes (**Fig. 6B** and Supplementary Fig. S7).

In spite of these results, Western blotting analysis using anti-CA antibody reveals an extremely low signal on the lane corresponding to CI subunits from *ca1ca3* sample (**Fig. 6B**, lower panel). This result suggests that there could be traces of assembled CI that are not detectable by colloidal Coomasie blue staining.

CI NADH DH activity level in *CA* mutants is tissue-dependent

In order to determine the relative contribution of each CA protein to CI activity, we isolated total membrane proteins

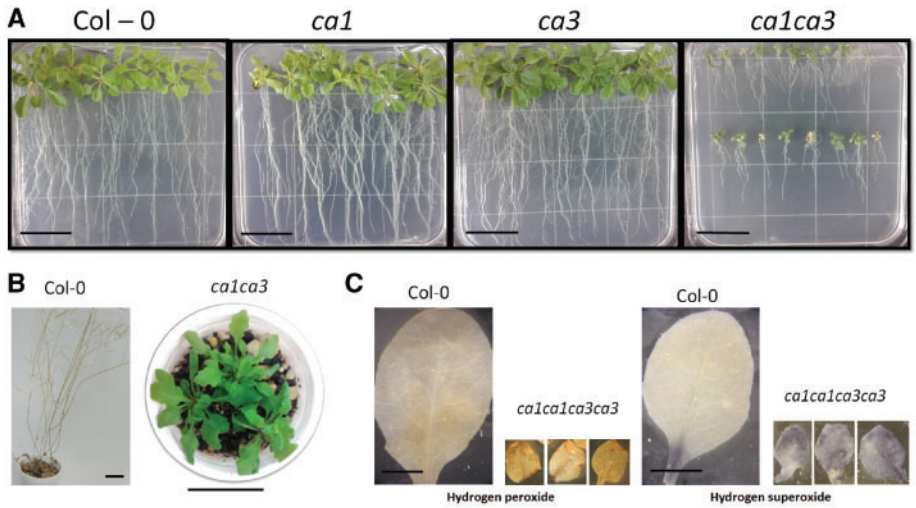

Fig. 5 *ca1ca3* rescued plants accumulate ROS. (A) Seeds from Col-0, *ca1*, *ca3* and shrunken *ca1ca3* were cultivated on 1% sucrose enriched MS medium. After 11 d, they were transferred to a 3% sucrose enriched medium and incubated 15 d more. Bars: 3 cm. (B) *ca1ca3* rescued plants were transferred to soil. Twenty-one days later were photographed. Bars: 3 cm. (C) Plants growth on MS medium as described were exposed to DAB and NBT staining in order to detect hydrogen peroxide and superoxide, respectively. Bars: 5 mm (Col-0) and 2 mm (*ca1ca3*).

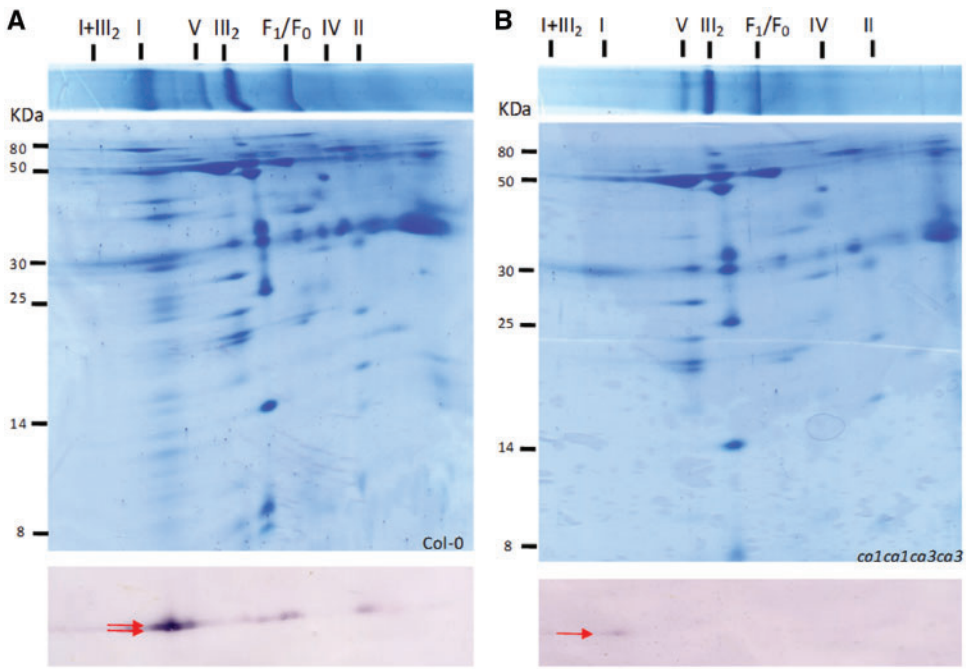

Fig. 6 CI is not detected by Coomasie blue in *ca1ca3* proteome. Mitochondria were isolated from cell cultures derived from Col-0 (A) and rescued *ca1ca3* plants (B). After solubilization, membrane protein complexes were separated on Blue Native PAGE (lane on the top of the figure). Then, one lane of each sample was separated on a second, denaturing dimension (SDS-PAGE) in order to disaggregate these complexes in their proteins (middle square). After second electrophoresis, gels were stained by colloidal Coomasie blue or transferred to nitrocellulose membranes to perform Western blotting analysis (bottom panel). Antibodies raised against gamma CAs were used to detect gamma CA proteins. Identity of each protein complex and molecular weight in the second dimension are indicated. Red arrows signalize gamma-CA detection.

from immature (pale, from globular to torpedo stages), mature (green) embryos and leaves of Col-0, *ca1*, *ca2* and *ca3* mutants. Proteins were then separated in a Blue Native PAGE and NADH DH activity of mitochondrial CI was measured (**Fig. 7**).

When CI NADH DH activity was analyzed in pale embryos, all three single mutants show a reduction of about 40%. At these stages of embryogenesis, *ca1* mutants seem to have more supercomplex activity (**Fig. 7A**). When green embryos were analyzed, *ca1* and *ca3* single mutants show a reduction of about 40% in comparison to Col-0, while *ca2* present a stronger reduction of around 60%. Unexpectedly, *ca1* and *ca3* mutants seem to have more activity of $I+III_2$ supercomplex than Col-0 (**Fig. 7B**).

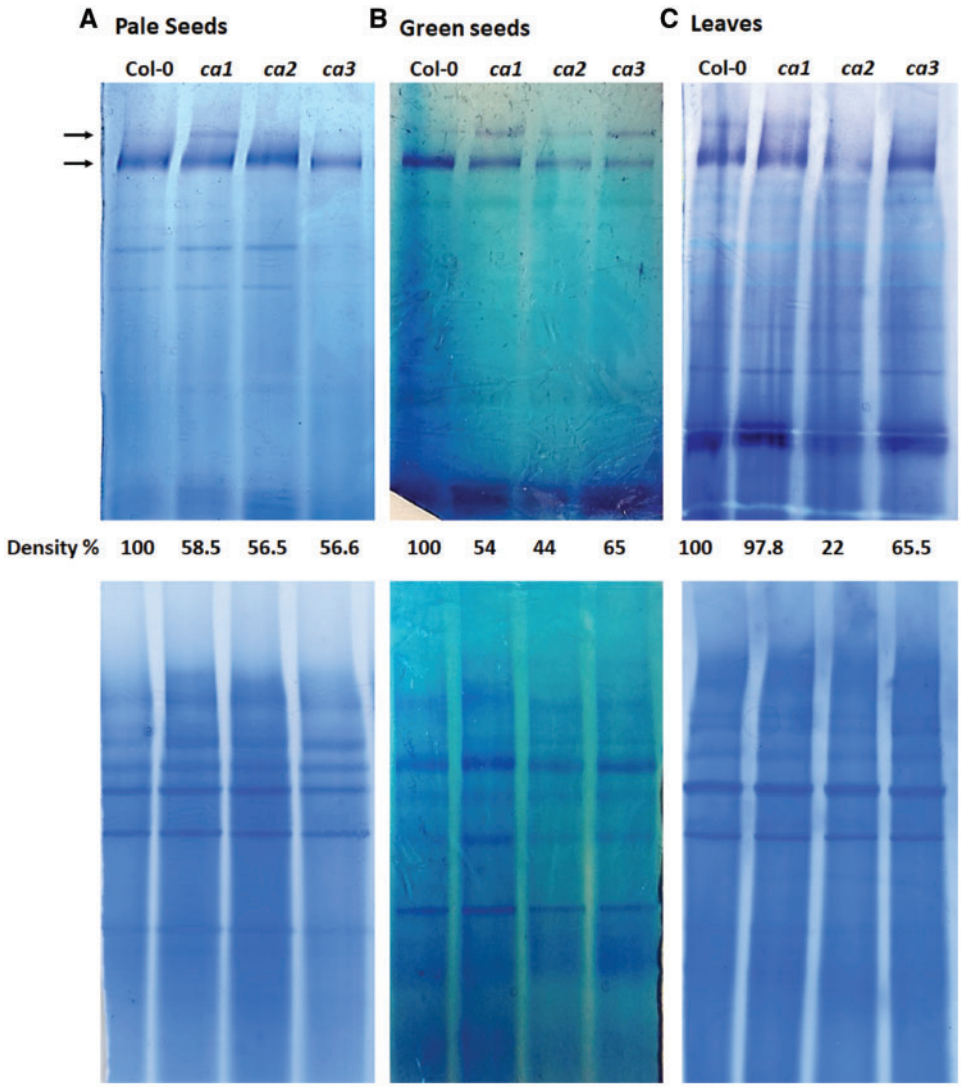

Fig. 7 CI activity in CA mutants is different among tissues. Membrane proteins from pale (A) and green (B) seeds, and leaves (C) corresponding to Col-0, *ca1*, *ca2* and *ca3* genotypes, were isolated and solubilized with digitonin. After Blue Native PAGE, in-gel NADH DH activity was determined. Representative gels are shown. Upper arrows indicate supercomplex I+III$_2$ position. Lower arrows indicate CI position. Numbers below indicate the quantification of CI by band density (in %) relative to loading taking from independent gels using the Image J software. Duplicates of each gel were stained with colloidal Coomasie blue G250 to use as loading controls (lower panel).

NADH DH activity of mitochondrial CI determined in leaves from plants grown in solid MS medium show a strong reduction (around 80%) in *ca2* mutants while *ca1* mutants show normal CI activity and *ca3* a mild reduction (around 35%) compared to Col-0 (**Fig. 7C**). These results confirm published data (Perales et al. 2005, Meyer et al. 2011, Soto et al. 2015, Córdoba et al. 2016) for leaves and cell suspension.

Thus, we conclude that the contribution of each CA protein to the assembly of an active CI differ depending the tissue or life cycle stage. While seems to be indistinctly during seed development, the contribution of the CA2 subunit is clearly the more important from green embryos on during embryogenesis and especially in leaves of adult plants.

CA3 can form homodimers and interacts with FRO1 in vivo

In the Arabidopsis Interactome Mapping (Braun et al. 2011) is suggested that the CA3 subunit was able to interact with some CA subunits. In order to test CA3 interaction partners, we performed Bimolecular Fluorescence Complementation (BiFC) assays in *Nicotiana benthamiana* epidermal cells. The CA3 coding sequence and those of all other CA family members were cloned into pH7FGW2 in order to make fusions to the N- or C-terminal fragments of Yellow Fluorescent Protein (YFP) (see M & M). The CA3-nYFP construct was transiently expressed in leaf cells of *N. benthamiana* alone or together with the tested proteins fused to the cYFP fragment by *Agrobacterium tumefaciens*-mediated leaf infiltration. BIFC

signal was visualized by confocal microscopy 72 h after infiltration. When CA3nYFP-CA3cYFP was assayed, YFP fluorescence was detected following a punctuated pattern consistent with an interaction (**Fig. 8A**). However, no BIFC signal was observed in leaves in which CA3-nYFP was co-expressed with CA1, CA2 or CALs-cYFP proteins (Supplementary Fig. S9). As expected, BIFC signal was observed for CA1-CA1 interaction (Supplementary Fig. S8; see Córdoba et al. 2016 for two-hybrid analysis). These experiments revealed that CA3 is able to interact with itself, but it is unable to interact with any other member of the CA family.

In the same in silico approach, it is also predicted that CA3 protein may interact with FRO1 (At5g67590), ND9 (AtMg00070) and ND6 (AtMg00270) among other CI subunits (Braun et al. 2011). To further test this possibility, a BIFC assay was performed. For the mitochondrial encoded genes, *ND6* and *ND9*, a mitochondrial signal peptide that was proved to address proteins to plant mitochondria (Hernould et al. 1993, Gómez-Casati et al. 2002, Busi et al. 2006) was used in their N-termini. For these mitochondrial proteins we were unable to detect expression after infiltration using similar constructs but fused to Green Fluorescent Protein (GFP) at their C-termini, thus we were unable to test these interactions. However, FRO1 and CA3 are able to interact in vivo, as BIFC signals were detected in both combinations (FRO1-cYFP with CA3-nYFP and FRO1-nYFP with CA3-cYFP) (**Fig. 8B, C**, respectively). Interestingly, the almost identical protein, CA1, neither interacts with CA3 nor with FRO1 (**Fig. 8D, E**), indicating that the CA3/FRO1 interaction is specific to CA3.

Double mutants *fro1ca3* show a stronger phenotype

To obtain independent data on the putative interaction between FRO1 and CA3, double *fro1ca3* knock out mutants were obtained. Single knock out *fro1* mutants show a number of unviable seeds while survival seedlings show a characteristic dwarf phenotype until maturity. It was previously shown that this particular mutant present traces of NADH DH activity and accumulates the membrane arm of CI (Kühn et al. 2015). In the double *fro1ca3* mutant, the number of unviable seeds increased significantly (from around 5% in the single *fro1* mutant to ~20% in the double mutant, $n = 150$). Moreover, the size of survival seedlings is slightly smaller than single *fro1* mutants (Supplementary Fig. S9). This result suggests that the lack of CA3 further destabilizes the subcomplex present in the *fro1* single mutant strengthening its already altered phenotype.

Discussion

Earlier reports showed specific roles for different members of the CA domain, suggesting their involvement during embryogenesis (Córdoba et al. 2016, Fromm et al. 2016a) and their roles in a photorespiratory context (Soto et al. 2015). In this work, we provide evidence about the different composition of complexes I through development and the role of the CA3 protein subunit in the assembly of CI. Taken together our results suggest that the first intermediate formed (i.e. the CA domain, Ligas et al. 2018) in the way of CI varies during the plant life cycle, presenting specific conformations along the different developmental stages. In pale embryos, CI may be formed from trimers containing indistinctly CA1-CA1-CAL, CA2-CA2-CAL or homotrimers of CA3. However, from green embryo stage on to adult plants, the CA2-CA2-CAL trimer becomes the more abundant (80% in the adult).

Complete lack of CI leads to embryo lethality

Many mutants affect CI assembly, directly by lacking an essential subunit or assembly factor or indirectly by lacking proteins important for maturation of mitochondrial RNAs coding for *nad* subunits. In Arabidopsis, the first mutant reported was *ca2* (Perales et al. 2005), which shows a reduction of fully assembled CI estimated in 80%. Also *ca3* mutant was affected, although

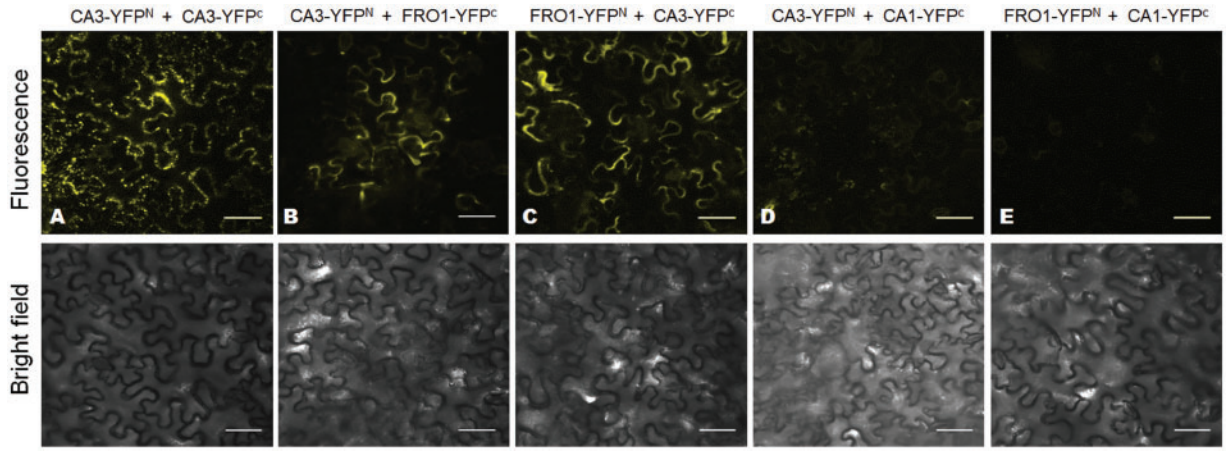

Fig. 8 CA3 protein is able to form homodimers and interacts FRO1 CI subunit in vivo. BiFC analysis of the interaction between CA3, CA1, ND6 and FRO1 proteins. Reconstituted YFP fluorescence or bright field images are shown in *N. benthamiana* epidermal leaf cells co-infiltrated with *A. tumefaciens* harboring the indicated constructs. (A) Representative images from confocal microscopy showing the interactions of CA3 with CA3, (B, C) interaction of CA3 with FRO1, in both directions, respectively. (D, E) Representative images from confocal microscopy showing that CA1 does not interact with CA3 nor FRO1 proteins. Bars: 50 μm.

with less severity. Other mutants like *ndufs4 (fro1)* and *ndufv1* (Meyer et al. 2009, Kühn et al. 2015) accumulate assembly intermediates of CI. While in *fro1*, traces of fully assembled CI with NADH DH activity are found, in *ndufv1*, NADH DH activity is not detected, although traces of a nearly complete assembled CI is also present (Ligas et al. 2018). Consequently, germination in the absence of sugar was not much affected in *ndufs4* mutants, while it is strongly affected and most seedlings died only in *ndufv1* mutants (Kühn et al. 2015). Some mutants lacking Pentatricopeptide Repeat Proteins, which are RNA binding proteins, with defects in splicing or stability of *nad* transcripts exhibit severely impaired CI assembly and activity, and show visual phenotypes such as reduced germination, retarded growth or curled leaves and in some cases embryo arrest phenotypes (OTP43, Falcon de Longevialle et al. 2007, PPR19, Lee et al. 2017, SLO3, Hsieh et al. 2015, MTSFs, Wang et al. 2017, Wang et al. 2018) depending on the remnant fully assembly CI present. Other CI mutants in nuclear maturase genes, like *nmat1* (Keren et al. 2012), *nmat2* (Keren et al. 2009) and *nmat4* (Cohen et al. 2014), all show a strong decrease in CI levels, although active traces are present and consequently mild phenotypes in all three mutants. Also in maize, four mutants, *emp8* (*EMPTY PERICARP 8*), *emp11*, *dek2* (*DEFECTIVE KERNEL2*) and *dek37* are strongly defective in seed development, which correlates with a defect in the splicing of some *nad* transcripts and strong decrease of fully assembled CI (Qi et al. 2017, Ren et al. 2017, Dai et al. 2018, Sun et al. 2018). Thus, only Arabidopsis mutants completely lacking fully assembled CI, like *ca1ca2* (Córdoba et al. 2016, Fromm et al. 2016a), *ca1ca3*—this work—*otp43* (Falcon de Longevialle et al. 2007) and *ndufv1* (Kühn et al. 2015, Ligas et al. 2018) do not survive on soil and require sucrose to germinate. Traces of CI might be enough in Arabidopsis but not in maize to achieve complete embryogenesis. These results indicate that the response of maize and Arabidopsis to altered CI assembly might be similar but with some variations. Maize embryos do not survive with traces of CI as Arabidopsis embryos do. An extreme opposite example constitutes *Viscum album*, which has a highly unusual OXPHOS system. It has recently been reported that the European mistletoe mitochondria completely lack CI and have greatly reduced amounts of complexes II and V. However, it only survives as an obligate semi-parasite, living on branches of trees. At the same time, the complexes III and IV form remarkably stable respiratory supercomplexes (Maclean et al. 2018, Senkler et al. 2018).

Double homozygous *ca1ca3 and ca2ca3* mutants are severely affected

In our work, the alleles used to generate the double homozygous *ca1ca3* show seedling lethality as was previously shown for *ca1ca2* (Córdoba et al. 2016). Although it was previously published that the double homozygous *ca1ca3* mutant does not show any phenotypical alteration compared to Col-0 plants (Wang et al. 2012, Senkler et al. 2017a), this discrepancy can be explained by the use of different mutant lines. In the first publication, the mutant alleles are not detailed; the origin or stock number of the mutant lines used is not specified as it is not shown whether they are null alleles.

Both CA double mutants (*ca1ca2* and *ca1ca3*) are lethal but can be rescued if grown in a medium enriched in sucrose. However, they show slight differences. Although developmental delay during embryogenesis is detected about 60 HAP in both mutants, MMP drops earlier in the *ca1ca3* genotype. In addition, *ca1ca3* embryos recover their mitochondrial potential from torpedo stage on, even when embryogenesis continues to be affected. We suggest that the apparent recovery of MMP could be due to a high induction of alternative electronic transport pathways (as alternative NADH DHs).

Both *ca1ca2* and *ca1ca3* mutant seedlings die soon after germination when not supplemented with sucrose (Córdoba et al. 2016, **Fig. 5**). Germination and seedling establishment are high energy demanding processes that depend only on compounds accumulated along embryogenesis, especially after embryo greening. As embryo development is delayed, *ca1ca2* and *ca1ca3* mutants never arrive to the greening stage. Consequently, it is possible that they might not be able to synthesize (or accumulate) enough lipids to sustain the entire process (Córdoba et al. 2016). Although *ca1ca2* (Fromm et al. 2016a) and *ca1ca3* adult plants can survive on soil after being rescued on sucrose, they do not have active CI and their energy transformation (from carbon to Adenosine Triphosphate (ATP)) efficiency is probably very low. Indeed, rescued plants are severely affected, showing high ROS accumulation (**Fig. 5**) and induction of alternative oxidases (Supplementary Fig. S7), responses that are very well known markers of a deficiency of CI activity (Falcon de Longevialle et al. 2007, Garmier et al. 2008, Keren et al. 2012, Hsu et al. 2014, Kühn et al. 2015, Fromm et al.2016c).

The differences observed between *ca1ca2* and *ca1ca3* double mutants could be explained by the presence of extremely low levels of CI in the latter. Indeed, traces of putative assembled CI were detected by Western blot after 2D BN/SDS-PAGE in *ca1ca3* mitochondria (**Fig. 6**). This suggested that although the assembly of CI might initiate with a CA domain composed by CA2 and CAL1/2 proteins, it would not be stable enough in a *ca3* mutant background. Since the transcript level of CA2 is almost unaffected (Supplementary Fig. S5B), we conclude that if translation is not affected, the leftover CA2 should be degraded.

To elucidate the basis of *ca2ca3* growth deficiencies, mutant plants were grown under a high CO_2 atmosphere (which is sufficient to rescue *ca2cal* photorespiratory mutants, Soto et al. 2015) or supplemented with sucrose (as lethal *ca1ca2*-Fromm et al. 2016a—and *ca1ca3* mutants—this work are rescued). However, these treatments were not enough to rescue the *ca2ca3* phenotype, suggesting that the severe growth deficiencies observed in *ca2ca3* mutants are at least not only due to photorespiratory or respiratory problems.

Expression of gamma CA members is tissue-specific

The promoter activity for each gamma CA member was analyzed using fusions with a reporter gene (Córdoba et al. 2016

and this work). Along embryogenesis, CA2 promoter was strongly active at late stages (mature green), while CA1 and CA3 promoter regions are more active in globular to heart stages. These differences might indicate a tissue-specific expression pattern and specific physiological roles of each gamma CA protein along embryo development.

It was previously suggested that the CA2 subunit may act as a CI assembly factor, essential for the initial steps of the assembly process (Meyer 2012). Thus, *ca2* null mutants show a strong reduction in CI abundance and NADH DH activity. However, this assumption was originated from results obtained from leaves or from cell suspensions derived from stem cells (Perales et al. 2005, Soto et al. 2015).

In a previous work (Córdoba et al. 2016), it was suggested that the formation of CI was dependent on CA2 or CA1. These proteins could form trimers with CAL proteins such as CA2-CA2-CAL (80%) or CA1-CA1-CAL (20%), because the CA3 subunit had not been detected in the 85 kDa CA domain extracted with low SDS (Klodmann et al. 2010). In light of recent works where CA3 was found first in a 130 kDa intermediate (Senkler et al. 2017b) and then in the 85 kDa intermediate (the first proposed intermediate for CI assembly, i.e. the CA domain) (Ligas et al. 2018), these ideas should be reinterpreted considering a proportion of CA3 dependent CI. Taking into account our results of interactions, where CA1 and CA2 proteins do not interact among them (Córdoba et al. 2016), the trimers might be CA2-CA2-CAL, CA1-CA1-CAL or homotrimers of CA3, because this last subunit does not interact with any other member of the CA family (this work). Furthermore, we show that NADH DH activity assays show that each single CA mutant is differently affected depending on the tissue and life cycle stage assayed. According to our results, during embryogenesis, assembly of CI seems to depend indistinctly on CA1, CA2 or CA3, which contrasts to the situation observed in mature plants where CA2 is the dominant subunit accounting for 80% of the trimers and consequently CI abundance. Surprisingly, *ca3* mutants show lower NADH DH activity in every tissue and stage compared to Col-0 (around 60%). These results suggest that gamma CA3 subunit is important for CI activity along all stages of the plant life cycle, probably contributing to CI stability as well.

The gamma CA3 subunit as a CI stabilization factor

In vivo interaction analysis revealed that the CA3 subunit was unable to interact with any other member of the CA family. An interpretation to explain these results is that a proportion of CI is dependent on homotrimers composed only by CA3 subunits. In that case, this proportion would be low, because *ca1ca2* and *cal1cal2* double mutants show embryo lethal phenotypes (Wang et al. 2012, Córdoba et al. 2016, Fromm et al. 2016a) and, at least in rescued *ca1ca2* lines, no traces of CI were observed. It is possible that the amount of CA3 dependent CI is might not be enough to sustain the embryogenesis and, in that context, be degraded. Even that, the difference between NADH DH activity seen in *ca3* leaves respect to Col-0 together with an increase in $I+III_2$ supercomplex activity, point to a stabilization role.

We suggest that the lack of CA3 leads to a destabilization of a proportion of CI, which is in turn detected as lower NADH DH activity in every tissue compared to Col-0, around 60%. In agreement with this idea, the absence of one of its putative interaction partners, FRO1, causes extremely low CI activity and accumulation of the membrane arm, as CI is not fully assembled (Meyer et al. 2009, Meyer et al. 2011). The phenotype of double mutants *fro1ca3* is stronger than the single *fro1* mutant, showing a 15% increase of unviable seeds and a slightly delay in the growing of the survival plants suggesting that the putative interaction between these two proteins might be important for CI assembly. An interpretation of these results might be that the proposed CA3 homotrimers should be able to interact with FRO1 in the matrix arm. However, as mentioned before, if that were the case, the proportion of CA3 homotrimers would be low, as *ca1ca2* and *cal1cal2* double mutants show embryo lethal phenotypes (Wang et al. 2012, Córdoba et al. 2016, Fromm et al. 2016a) and *ca1ca2* lines show no traces of CI. A second interpretation could be to consider the existence of a homotrimer of CA3 located outside the CA domain, interacting with at least FRO1 and having a role of complex and supercomplex stability. This putative homotrimer of CA3 might have a similar size to the CA domain and if it is not stably bonded, might be detached during purification, migrating at a similar position to the 85 kDa intermediates when analyzed on gels (Ligas et al. 2018). The fact that a complex CA3-FRO1 was not detected in the mass spectrometry experiments of Ligas et al. (2018) or Senkler et al. (2017b) points to an instability of this putative interaction. This interpretation may explain the similar decrease of NADH DH activity observed regardless on the tissue and the increase of supercomplex ($I+III_2$) detected in the *ca3* single mutant, however, these results based on BIFC experiments should be taken with care, as some in vivo interactions may not be visualized using this method. In spite of the high sequence similarity among gamma CA members, especially between CA1 and CA3 (77% aminoacid sequence identity), the differences found in this work point to a functional and/or physiological specialization of each member of this protein family in *A. thaliana*.

Materials and Methods

Plant material and cell cultures

Long-day conditions were established at 16:8 h (L:D), 120 μE light intensity and 22°C. Short-day conditions were 10:14 h (L:D), 120 μE light intensity and 22°C. *Arabidopsis thaliana* Ecotype Columbia-0 and the mutants were growth on soil or in plate (with Murashige and Skoog medium supplemented with Gamborg's Vitamins (Sigma) and with or without sucrose as indicated). For selection of transgenic lines, Hygromycin (Sigma) 15 μg/ml was added to MS medium. Seeds cultivated on plates were previously surface sterilized with 50% v/v ethanol during 10 min and then with isopropanol, 30 min with constant shaking. After this time, they were washed five times with sterile water. Double mutants were obtained by cross pollination between single null mutants: *ca1* (Salk_109391), *ca2* (Salk_010194), *ca3* (CS69934), *fro1* (SAIL_596_E11). Cell cultures were established as described in Perales et al. (2005). See Supplementary Fig. S1 for alleles and the structure of genes used in this work and positions of T-DNA insertions.

The *ca3* mutant was complemented using a construct with a 1,500 bp *ca3* promoter and the Coding sequence (CDS) of the *ca3* gene to distinguish from the WT sequence. Since *ca3* mutants show lower NADH DH activity (around 65%), we measured this activity in complemented lines. Restored NADH DH activity was seen in complemented lines. Supplementary Fig. S10 shows a representative complemented line compared to Col-0 and *ca3* mutant.

Genotyping of mutant lines

T-DNA insertional mutants or derived cell suspension cultures used in this work were genotyped by detection of mutated alleles. For Salk lines, a combination of LBb1.3 oligo (5′-ATTTTGCCGATTTCGGAAC-3′) and corresponding Fw (CA1 Fw: 5′-ATCTCGAGATGGGAACCCTAGGCA-3′; CA2 Fw: 5′-CACTCG AGTGGGAACCCTAGGA-3′). For *ca3* mutation, SynLB1 oligo (5′- GCCTTTTCA GAAATGGATAAATAGCCTTGCTTCC-3′) and CA3 Rv (5′-ATCTCGAGTCAAG CTGCTTTTGGT-3′) were used. Wild type alleles were detected by combination of CA1Fw/CA1Rv (5′-CACACCACCTCCAATACTTTCAGCC-3′), CA2Fw/ CA2Rv (5′- TCAGAGTAGGTAGAACCTTGCCA-3′) and CA3Fw (5′- GCCTCG AGATGAATGTTTTTGAC-3′)/CA3Rv.

Phenotype analysis

Visualization of *ca1ca3* seed sets, embryo stages along embryogenesis taken by Differential interference contrast (DIC) optics and MMP status detected by staining with TetraMethylRhodamine (TMRM) were conducted as previously described (Córdoba et al. 2016). Quantification of red fluorescence intensity was measured following standardized protocols (Martin et al. 2014, Córdoba et al. 2016).

Promoter activity

Promoter regions taken as sequences upstream first translational first codon (ATG) codon were cloned into pMDC162 vector (Curtis and Grossniklaus 2003). Col-0 plants were transformed with Promoter::*GUS* constructs by floral dip method (Clough and Bent 1998). Two thousand basis pair for CA1 and 1,470 bp for CA3 were analyzed by GUS staining as described in Córdoba et al. (2016) for CA2 promoter activity.

ROS detection

In order to detect hydrogen peroxide and hydrogen superoxide, plant leaves were stained with diaminobenzidine (DAB) and NitroblueTetrazolium (NBT), respectively. For DAB staining, leaves were incubated in total darkness with 1 mg/ml solution in (pH 3 water) along 12 h. After that, samples were washed with distilled water and chlorophyll were extracted by discoloration in 96% v/v ethanol, in constantly shaking. Then, leaves were washed with water. *In situ* brown staining was observed. NBT staining was conducted by incubation of leaves in 10 mM phosphate buffer pH 8, 10 mM NaN_3 and 0.1% NBT (Sigma), along 12 h at 37°C. Washing and chlorophyll discoloring were performed as described by DAB. *In situ* superoxide was detected by violet staining.

RT-qPCR transcription measurements

Total RNA from Col-0 and *ca1ca3* double homozygous mutants was isolated by TRIzol reagent (Invitrogen) and used in retrotranscriptase reactions (with Promega enzymes and random hexamers). cDNA was then used in qPCR reaction using Power SyBR mix (AppliedBiosystems) in a StepOnethermocycler. qPCRoligos pairs were used as in Soto et al. (2015). Transcript levels were normalized against ACT2 and UBQ5 as housekeeping genes.

2D Blue Native/SDS-PAGE

Isolation of mitochondria from cell cultures was carried out following the protocol described in Perales et al. (2005). Mitochondrial membrane protein complexes were solubilized in digitonin. Ten micrograms of mitochondria (around 1 mg mitochondrial proteins) were mixed and incubated with 2.5 mg of digitonin in 100 µl (Eubel et al. 2003) previous to electrophoresis separation. One-dimension blue native electrophoresis was performed as described in Wittig et al. (2006), in large, polyacrylamide gradient (4 to 16% p/v) gels. After 18 h running at 500V, 15 mA, lanes were stained overnight in colloidal Coomasie blue G-250. Duplicated lanes were properly cut and mounted horizontally in a 16% polyacrylamide gel (Wittig et al. 2006). Protein complexes were thus separated in their proteins after 20 h running at 500 V, 25 mA in denaturing conditions (SDS). After running, proteins spots were detected by staining in colloidal Coomasie blue G-250, overnight.

Mitochondrial membrane protein complexes from embryos or plants (leaves and roots) were isolated as is outlined in Pineau et al. (2008). After that, proteins were separated as described above.

NADH DH activity staining

Separation of protein complexes under native conditions allows in-gel activity staining. NADH DH activity was assayed incubating the gels with 0.14 mM NADH (sigma) and 1 mg/ml NBT in 0.1 M Tris–HCl pH 7.4 until violet band is clearly viewed. After that, gels were fixed in 40% v/v methanol, 10% v/v acetic acid.

Protein immune detection

We used an anti-CAs serum to detect γCA1, γCA2 and γCA3 proteins. Mitochondrial proteins separated by 2D BN/SDS-PAGE were transferred to nitrocellulose membranes (GE Healthcare) and incubated with these primary antibody and then with an anti-rabbit secondary antibody (Sigma) conjugated with alkaline phosphatase, following standard protocols. Final development was carried out with NBT/BCiP (Promega).

Immune detection of alternative oxidase isoforms was performed on proteins obtained from Col-0 and *ca1ca3* (rescued) plants. After mitochondrial membrane protein complexes solubilization in digitonin, proteins were treated under denaturing conditions (5 min at 98°C heating and β-mercaptoethanol), and then, separated in 12% polyacrylamide SDS-PAGE. Protein transfer and immunodetection were performed as described above. Anti-Alternative Oxidase (AOX) primary polyclonal antibodies are from Agrisera (Sweden; Catalog AS04 054).

BiFC in vivo interactions

In vivo analysis of protein interaction was performed by Bimolecular Fluorescence Complementation (BiFC) assay. The cDNA sequences of CA1, CA2, CA3, CAL1, CAL2, FRO1 (At5g67590, other name NDUFS4) and ND6(AtMg00270) were PCR amplified using the following primers: **CA1** (5′-C ACCATGGGAACCCTAGGCAGA-3′/5′-GTTCACATTAGAAGGACGCTT-3′), **CA2** (5′-CACCATGGGAACCCTAGGACGA-3′/5′-GAAGTACTGGATAGAC GGAAC-3′), **CA3** (5′-CACCATGGGAACAATGGGTAAA-3′/5′-AGGTGCTTT TGGTACATTCTC-3′), **CAL1** (5′-CACCATGGCGACTTCGATAGCT-3′/5′-TA AACGGCGATCCCAAGGGAC-3′), **CAL2** (5′-CACCATGGCGACTTCGTT AGCA-3′/5′-GATGGCGATTCCAAGGGATTT-3′), **FRO1** (5′-CACCATGGCG CTTTGTGCT-3′/5′-GTTTTCTGGTTGAGGATT3′) and **ND6** (5′-CACCATG ATACTTTCTGTT-3′/5′-GTAGATCGTTGGGTC-3′). The PCR product were cloned into pENTR TOPO plasmids using Gateway technology (Invitrogen), sequenced and recombined through BP reaction into pH7FGW2 destination vector (half YFP C-t; Grefen et al. 2010). The binary plasmids were then transformed into *A. tumefaciens* strain GV3101 by electroporation. Split tagged protein -nYFP and tagged protein -cYFP pairs were co-expressed in young (4–5 weeks) *N. benthamiana* leaves by *A. tumefaciens*-mediated inoculation. Plant leaves were examined 72 h post-infiltration with a confocal microscope (Nikon Eclipse C1 Plus).

Supplementary Data

Supplementary data are available at PCP online.

Funding

Agencia Nacional de Promoción Científica y Tecnológica (ANPCyT), Consejo Nacional de Investigación Científica y Tecnológica (CONICET) and Howard Hughes Medical Institute (HHMI).

Acknowledgments

J.P.C. and M.F. are postdoctoral fellows, and F.M. is a doctoral fellow of the Consejo Nacional de Investigaciones Científicas y Técnicas (CONICET). G.C.P. and E.J.Z. are CONICET researchers. This work was supported by Agencia Nacional de Promoción Científica y Técnica (ANPCyT, PICT'16 0036), CONICET and the Howard Hughes Medical Institute (HHMI). We are grateful to Daniela Villamonte for excellent technical assistance with confocal microscopy.

Disclosures

The authors have no conflicts of interest to declare.

References

Baradaran, R., Berrisford, J.M., Minhas, G.S. and Sazanov, L.A. (2013) Crystal structure of the entire respiratory complex I. *Nature* 494: 443–448.

Berrisford, J.M., Baradaran, R. and Sazanov, L.A. (2016) Structure of bacterial respiratory complex I. *Biochim. Biophys. Acta.* 1857: 892–901.

Braun, P., Carvunis, A.R. and Charloteaux, B. (2011) Evidence for network evolution in an Arabidopsis interactome map. *Science* 333: 601–607.

Busi, M.V., Gómez-Casati, D.F., Perales, M., Araya, A. and Zabaleta, E. (2006) Nuclear-encoded mitochondrial complex I gene expression is restored to normal levels by inhibition of unedited ATP9 transgene expression in *Arabidopsis thaliana*. *Plant Physiol. Biochem*. 44: 1–6.

Cardol, P. (2011) Mitochondrial NADH: ubiquinone oxidoreductase (complex I) in eukaryotes: a highly conserved subunit composition highlighted by mining of protein databases. *Biochim. Biophys. Acta* 1807: 1390–1397.

Clough, S.J. and Bent, A.F. (1998) Floral dip: a simplified method for *Agrobacterium*-mediated transformation of *Arabidopsis thaliana*. *Plant J.* 16: 735–743.

Cohen, S., Zmudjak, M., Colas Des Francs-Small, C., Malik, S., Shaya, F., Keren, I., et al. (2014) nMAT4, a maturase factor required for nad1 pre-mRNA processing and maturation, is essential for holocomplex I biogenesis in Arabidopsis mitochondria. *Plant J.* 78: 253–268.

Córdoba, J.P., Marchetti, F., Soto, D., Martin, V., Pagnussat, G.C. and Zabaleta, E. (2016) The CA domain of the respiratory complex I is required 1 for normalembryogenesis in *Arabidopsis thaliana*. *J. Exp. Bot.* 67: 1589–1603.

Curtis, M.D. and Grossniklaus, U. (2003) A gateway cloning vector set for high-throughput functional analysis of genes in planta. *Plant Physiol.* 133: 462–469.

Dai, D., Luan, S., Chen, X., Wang, Q., Feng, Y., Zhu, C., et al. (2018) Maize Dek37 Encodes a P-type PPR protein that affects cis-splicing of mitochondrial nad2 intron 1 and seed development. *Genetics* 208: 1069–1082.

Dudkina, N.V., Eubel, H., Keegstra, W., Boekema, E.J. and Braun, H.-P. (2005) Structure of a mitochondrial supercomplex formed by respiratory-chain complexes I and III. *Proc. Natl. Acad. Sci. USA* 102: 3225–3229.

Eubel, H., Jänsch, L. and Braun, H.-P. (2003) New insights into the respiratory chain of plant mitochondria. Supercomplexes and a unique composition of complex II. *Plant Physiol*. 133: 274–286.

Falcon de Longevialle, A., Meyer, E.H., Andrés, C., Taylor, N.L., Lurin, C., Millar, A.H., et al. (2007) The pentatricopeptide repeat gene OTP43 is required for trans-splicing of the mitochondrial nad1 Intron 1 in *Arabidopsis thaliana*. *Plant Cell* 19: 3256–3265.

Fromm, S., Braun, H.-P. and Peterhänsel, C. (2016a) Mitochondrial gamma carbonic anhydrases are required for complex I assembly and plant reproductive development. *New Phytol.* 211: 194–1207.

Fromm, S., Göing, J., Lorenz, C., Peterhänsel, C. and Braun, H.-P. (2016b) Depletion of the "gamma-type carbonic anhydrase-like" subunits of complex I affects central mitochondrial metabolism in *Arabidopsis thaliana*. *Biochim. Biophys. Acta* 1857: 60–71.

Fromm, S., Senkler, J., Eubel, H., Peterhänsel, C. and Braun, H.-P. (2016c) Life without complex I: proteome analyses of an Arabidopsis mutant lacking the mitochondrial NADH dehydrogenase complex. *J. Exp. Bot.* 67: 3079–3093.

Garmier, M., Carrol, A.J., Delannoy, E., Vallet, C., Day, D.A., Small, I.D., et al. (2008) Complex I dysfunction redirects cellular and mitochondrial metabolism in Arabidopsis. *Plant Physiol*. 148: 1324–1341.

Gómez-Casati, D.F., Busi, M.V., Gonzalez-Schain, N., Mouras, A., Zabaleta, E.J. and Araya, A. (2002) A mitochondrial dysfunction induces the expression of nuclear-encoded complex I genes in engineered male sterile *Arabidopsis thaliana*. *FEBS Lett*. 532: 70–74.

Grefen, C., Chen, Z., Honsbein, A., Donald, N., Hills, A. and Blatt, M.R. (2010) A novel motif essential for SNARE interaction with the K+ channel KC1 and channel gating in Arabidopsis. *Plant Cell* 22: 3076–3092.

Hernould, M., Suharsono, S., Litvak, S., Araya, A. and Mouras, A. (1993) Male-sterility induction in transgenic tobacco plants with an unedited atp9 mitochondrial gene from wheat. *Proc. Natl. Acad. Sci. USA* 90: 2370–2374.

Hsieh, W.Y., Liao, J.C., Chang, C.Y., Harrison, T., Boucher, C. and Hsieh, M.H. (2015) The SLOW GROWTH3 pentatricopeptide repeat protein is required for the splicing of mitochondrial NADH dehydrogenase subunit7 intron 2 in Arabidopsis. *Plant Physiol.* 168: 490–501.

Hsu, Y.W., Wang, H.J., Hsieh, M.H., Hsieh, H.L. and Jauh, G.Y. (2014) Arabidopsis mTERF15 is required for mitochondrial nad2 intron 3 splicing and functional complex I activity. *PLoS One* 9: e112360.

Keren, I., Bezawork-Geleta, A., Kolton, M., Maayan, I., Belausov, E., Levy, M., et al. (2009) AtnMat2, a nuclear-encoded maturase required for splicing of group-II introns in Arabidopsis mitochondria. *RNA* 15: 2299–2311.

Keren, I., Tal, L., Colas Des Francs-Small, C., Araújo, W.L., Shevtsov, S., Shaya, F., et al. (2012) nMAT1, a nuclear-encoded maturase involved in the trans-splicing of nad1 intron 1, is essential for mitochondrial complex I assembly and function. *Plant J.* 71: 413–426.

Klodmann, J., Sunderhaus, S., Nimtz, M., Jänsch, L. and Braun, H.-P. (2010) Internal architecture of mitochondrial complex I from *Arabidopsis thaliana*. *Plant Cell* 22: 797–810.

Kühn, K., Obata, T., Feher, K., Bock, R., Fernie, A.R. and Meyer, E.H. (2015) Complete mitochondrial complex I deficiency induces an up-regulation of respiratory fluxes that is abolished by traces of functional complex I. *Plant Physiol.* 168: 1537–1549.

Lee, K., Han, J.H., Park, Y.I., Colas Des Francs-Small, C., Small, I. and Kang, H. (2017) The mitochondrial pentatricopeptide repeat protein PPR19 is involved in the stabilization of NADH dehydrogenase 1 transcripts and is crucial for mitochondrial function and *Arabidopsis thaliana* development. *New Phytol.* 215: 202–216.

Ligas, J., Pineau, E., Bock, R., Huynen, M.A. and Meyer, E.H. (2018) The assembly pathway of complex I in *Arabidopsis thaliana*. *Plant J.* doi: 10.1111/tpj.14133.

Martin, M.V., Villarreal, F., Miras, I., Navaza, A., Haouz, A., Gonzalez-Lebrero, R., et al. (2009) Recombinant plant gamma carbonic anhydrase homotrimers bind inorganic carbon. *FEBS Lett*. 583: 3425–3430.

Martin, M.V., Fiol, D.F., Zabaleta, E.J. and Pagnussat, G.C. (2014) *Arabidopsis thaliana* embryo sac mitochondrial membrane potential stain. *Bioprotocols* 4: e1128.

Maclean, A.E., Hertle, A.P., Ligas, J., Bock, R., Balk, J. and Meyer, E.H. (2018) Absence of complex i is associated with diminished respiratory chain function in European mistletoe. *Curr. Biol*. 28: 1614–1619.

Meyer, E.H., Tomaz, T., Carroll, A.J., Estavillo, G., Delannoy, E., Tanz, S.K., et al. (2009) Remodeled respiration in ndufs4 with low phosphorylation efficiency suppresses Arabidopsis germination and growth and alters control of metabolism at night. *Plant Physiol*. 151: 603–619.

Meyer, E.H., Solheim, C., Tanz, S.K., Bonnard, G. and Millar, A.H. (2011) Insights into the composition and assembly of the membrane arm of plant complex I through analysis of subcomplexes in *Arabidopsis* mutant lines. *J. Biol. Chem.* 286: 26081–26092.

Meyer, E.H. (2012) Proteomic investigations of complex I composition: how to define a subunit? *Front. Plant Sci.* 3: 1–7.

Ostersetzer-Biran, O. (2016) Respiratory complex I and embryo development. *J. Exp. Bot.* 67: 1205–1207.

Parisi, G., Perales, M., Fornasari, M., Colaneri, A., Schain, N., Casati, D., et al. (2004) Gamma carbonic anhydrases in plant mitochondria. *Plant Mol. Biol.* 55: 193–207.

Perales, M., Eubel, H., Heinemeyer, J., Colaneri, A., Zabaleta, E. and Braun, H.-P. (2005) Disruption of a nuclear gene encoding a mitochondrial gamma carbonic anhydrase reduces complex I and supercomplex $I+III_2$ levels and alters mitochondrial physiology in Arabidopsis. *J. Mol. Biol.* 350: 263–277.

Perales, M., Parisi, G., Fornasari, M.S., Colaneri, A., Villarreal, F., González-Schain, N., et al. (2004) Gamma carbonic anhydrase like complex interact with plant mitochondrial complex I. *Plant Mol. Biol.* 56: 947–957.

Peters, K., Dudkina, N., Jänsch, L., Braun, H.-P. and Boekema, E.J. (2008) A structural investigation of complex I and I+III2 supercomplex from *Zea mays* at 11–13 Å resolution: assignment of the carbonic anhydrase domain and evidence for structural heterogeneity within complex I. *Biochim. Biophys. Acta* 1777: 84–93.

Pineau, B., Layoune, O., Danon, A. and De Paepe, R. (2008) L-galactono-1, 4-lactone dehydrogenase is required for the accumulation of plant respiratory complex I. *J. Biol. Chem.* 47: 32500–32505.

Qi, W., Yang, Y., Feng, X., Zhang, M. and Song, R. (2017) Mitochondrial function and maize kernel development requires Dek2, a pentatricopeptide repeat protein involved in nad1 mRNA splicing. *Genetics* 205: 239–249.

Ren, X., Pan, Z., Zhao, H., Zhao, J., Cai, M., Li, J., et al. (2017) EMPTY PERICARP11 serves as a factor for splicing of mitochondrial nad1 intron and is required to ensure proper seed development in maize. *J. Exp. Bot.* 68: 4571–4581.

Senkler, J., Senkler, M. and Braun, H.-P. (2017a) Structure and function of complex I in animals and plants—a comparative view. *Physiol. Plant.* 161: 6–15.

Senkler, J., Senkler, M., Eubel, H., Hildebrandt, T., Lengwenus, C., Schertl, P., et al. (2017b) The mitochondrial complexome of *Arabidopsis thaliana*. *Plant J.* 89: 1079–1092.

Senkler, J., Rugen, N., Eubel, H., Hegermann, J. and Braun, H.-P. (2018) Absence of complex I implicates rearrangement of the respiratory chain in European mistletoe. *Curr. Biol.* 28: 1606–1613.

Subrahmanian, N., Remacle, C. and Hamel, P.P. (2016) Plant mitochondrial complex I composition and assembly: a review. *Biochim. Biophys. Acta* 1857: 1001–1014.

Sun, F., Zhang, X., Shen, Y., Wang, H., Liu, R., Wang, X., et al. (2018) The pentatricopeptide repeat protein EMPTY PERICARP8 is required for the splicing of three mitochondrial introns and seed development in maize. *Plant J.* 95: 919–932.

Soto, D., Córdoba, J.P., Villarreal, F., Bartoli, C., Schmitz, J., Maurino, V., et al. (2015) Functional characterization of mutants affected in the carbonic anhydrase domain of the respiratory complex I in *Arabidopsis thaliana*. *Plant J.* 83: 831–844.

Stroud, D.A., Surgenor, E.E., Formosa, L.E., Reljic, B., Frazier, A.E., Dibley, M.G., et al. (2016) Accessory subunits are integral for assembly and function of human mitochondrial complex I. *Nature* 538: 123–126.

Villarreal, F., Martín, M.V., Colaneri, A., Gonzalez-Schain, N., Perales, M., Martin, M., et al. (2009) Ectopic expression of mitochondrial gamma carbonic anhydrase 2 causes male sterility by anther indehiscence. *Plant Mol. Biol.* 70: 471–485.

Wang, C., Aubé, F., Planchard, N., Quadrado, M., Dargel-Graffin, C., Nogué, F., et al. (2017) The pentatricopeptide repeat protein MTSF2 stabilizes a nad1 precursor transcript and defines the 3′ end of its 5′-half intron. *Nucleic Acids Res.* 45: 6119–6134.

Wang, C., Aubé, F., Quadrado, M., Dargel-Graffin, C. and Mireau, H. (2018) Three new pentatricopeptide repeat proteins involved in splicing of mitochondrial transcripts and complex I biogenesis in *Arabidopsis thaliana*. *J. Exp. Bot.* 69: 5131–5140.

Wang, Q., Fristedt, R., Yu, W., Chen, Z., Liu, H., Lee, Y., et al. (2012) The gamma-carbonic anhydrase subcomplex of mitochondrial complex I is essential for development and important for photomorphogenesis of Arabidopsis. *Plant Physiol.* 160: 1373–1383.

Wittig, I., Braun, H.-P. and Schägger, H. (2006) Blue-native PAGE. *Nat. Protoc.* 1: 418–428.